HHS Public Access

Author manuscript

Magn Reson Med. Author manuscript; available in PMC 2020 August 01.

Published in final edited form as:

Magn Reson Med. 2019 August ; 82(2): 658–670. doi:10.1002/mrm.27752.

Assessing test-retest reliability of phase contrast MRI for measuring cerebrospinal fluid and cerebral blood flow dynamics

Ashwin R Sakhare[1,2], **Giuseppe Barisano**[2,3], and **Judy Pa**[1,2,3]

[1]Department of Biomedical Engineering, Viterbi School of Engineering, University of Southern California, Los Angeles, USA

[2]Department of Neurology, Laboratory of Neuro Imaging, Stevens Neuroimaging and Informatics Institute, University of Southern California, Los Angeles, USA

[3]Neuroscience Graduate Program, University of Southern California, Los Angeles, USA

Abstract

PURPOSE: Pathological states occur when cerebrospinal fluid (CSF) and cerebral blood flow (CBF) dynamics become dysregulated in the brain. PC-MRI is a non-invasive imaging technique that enables quantitative measurements of CSF and CBF flow. While studies have validated PC-MRI as an imaging technique for flow, few studies have evaluated its reliability for CSF and CBF flow parameters commonly associated with neurological disease. The purpose of this study was to evaluate test-retest reliability at the cerebral aqueduct (CA) and C2-C3 area using PC-MRI to assess the feasibility of investigating CSF and CBF flow dynamics.

METHODS: This study was performed on 27 cognitively normal young adults (ages 20–35). Flow data was acquired on a 3T Siemens Prisma using a 2D cine-PC pulse sequence. Three consecutive flow measurements were acquired at the CA and C2-C3 area. Intraclass correlation (ICC) and coefficient of variance (CV) were used to evaluate intra-rater, inter-rater, and test-retest reliability.

RESULTS: Among the 26 flow parameters analyzed, 22 had excellent reliability (ICC>0.80), including measurements of CSF stroke volume, flush peak, and fill peak, and 4 parameters had good reliability (ICC 0.60–0.79). 16 flow parameters had a mean CV≤10%, 7 had a CV≤15%, and 3 had a CV≤30%. All CSF and CBF flow measurements had excellent inter-rater and intra-rater reliability (ICC>0.80).

CONCLUSION: This study shows that CSF and CBF flow can be reliably measured at the CA and C2-C3 area using PC-MRI, making it a promising tool for studying flow dynamics in the central nervous system.

Keywords

brain; cerebral blood flow dynamics; cerebrospinal fluid flow dynamics; phase-contrast MRI; test-retest reliability

Corresponding Author: Judy Pa, PhD, Laboratory of Neuro Imaging, Stevens Neuroimaging and Informatics Institute, University of Southern California, 2025 Zonal Ave, Los Angeles, CA 90033, 323-442-7246 (phone), jpa@ini.usc.edu.

INTRODUCTION

The continuous circulation of cerebrospinal fluid (CSF) and cerebral blood flow (CBF) is key to the health of our central nervous system. CBF provides oxygen and glucose to support the high metabolic demands of the brain and plays a key role in sustaining localized neuronal activity through neurovascular coupling.[1] CSF provides buoyancy to cushion the brain from injury, distributes neurotrophic factors, and stabilizes pH and chemical gradients.[2] CSF and CBF also support waste removal from the CNS through the blood brain barrier, glymphatic, and perivascular clearance pathways.[3]

Indeed, when CSF and CBF dynamics in the brain become dysregulated, pathophysiological states occur that have been associated with communicating and normal pressure hydrocephalus[4,5,6,7,8], syringomyelia[9,10], and Chiari malformations[11,12,13,14]. For example, individuals with Chiari malformations have decreased CSF velocity and shorter periods of caudal CSF flow at the cranio-cervical junction compared to normal controls.[15] Other diseases have recently shown evidence of CSF and CBF dysregulation, such that mild cognitive impairment (MCI) patients have shown higher arterial pulsatility, pulse volume, and CBF flow[17], and Alzheimer's disease (AD) patients have shown lower arterio-venous delays[17] when compared to age-matched normal controls. Taken together, these studies suggest that brain flow dynamics may be an important biomarker for identifying meaningful alterations in neurological diseases.

Using phase-contrast MRI (PC-MRI), a validated, non-invasive imaging technique, rapid measurements of CSF and CBF flow in the brain can be quantitatively assessed.[18,19,20] Furthermore, by coupling the measurement with a peripheral pulse transducer, CSF and CBF flow acquisition can be synchronized to the cardiac cycle, allowing for more accurate physiological interpretations.[4] However, while PC-MRI has shown a lot of utility in measuring flow, there are several potential sources of error that can significantly affect the accuracy and precision of this technique, including slice orientation, the velocity encoding value, complexity of the ROI, partial volume effects, and intra-voxel dephasing.[21,22,23,24,25] Gradient non-linearities, concomitant gradients (Maxwell terms), and eddy-current field errors are also major sources of inaccuracies in flow measurements.[23,24,25,26,27]

Gradient non-linearities are caused by geometric limitations in the gradient coils, which result in unwanted higher order, nonlinear encoding gradients.[30] Concomitant gradients are nonlinear, spatially-dependent magnetic fields that are generated when a linear magnetic field gradient is activated.[28,29,30] Gradient non-linearities and concomitant gradients both cause phase errors but can be corrected for and eliminated during image reconstruction without user intervention.[28,31] Eddy currents are created from rapidly switching the velocity encoding gradient during acquisition. This switching causes a change in the magnetic flux at the gradient coils, leading to spatially varying phase errors on the image.[29,32] The magnitude of these eddy currents are based on the flow velocity at the region of interest, as regions with slow flow require stronger encoding gradients resulting in larger field distortions.[29] Eddy currents that cannot be compensated for by the pre-emphasis system will result in a velocity offset in the background (stationary tissue) pixels on the image.[33] Regions with CSF flow are most susceptible to these effects as peak velocities are usually less than 20 cm/s, and

often on the order of 1–2 cm/s, while blood flow velocities are typically between 50–300 cm/s.[34]

Previous studies evaluating PC-MRI flow measurement accuracy and precision on phantoms have shown variable results based on vessel diameter and flow rate. In one study, phantom flow velocities between 0.8 cm/s and 25.4 cm/s resulted in an average measurement error for accuracy of 21% and CV of 3%. However, at the low end of this velocity range (<12 cm/s), PC-MRI significantly overestimated flow velocities and had reduced reproducibility.[34] In another study, it was shown that PC-MRI had good reproducibility but overestimated peak systolic and diastolic flow by approximately 35% when the phantom vessel diameter was 2 mm, a physiologically normal size for the CA.[35] This was attributed to partial volume effects at the boundaries.[35] At larger diameters of 4 mm and 6 mm, such as those often seen in individuals with NPH, the measured flow rates were similar to the true phantom flow rates.[35] In the same study, it was also shown that flow could reliably be measured in vivo at the CA with CVs < 9%.[35] Overall, this suggests that accuracy, and to a lesser extent precision, is significantly affected by vessel diameter and flow rate, likely due to a combination of the sources of error described above.

Several of the studies described above have validated PC-MRI as a reliable imaging technique for flow in phantoms[25] as well as CSF and CBF flow in the human brain.[27,36,37] However, many of these studies have not comprehensively evaluated test-retest, intra-rater, and inter-rater reliability for biologically-relevant parameters related to CSF and CBF time, flow rate, pulsatility, and volume, which have been measured in research studies of neurological diseases.[16,17,38,39] Therefore, in this study, we evaluated test-retest, intra-rater, and inter-rater reliability for 26 comprehensive measurements of flow at the cerebral aqueduct and cervical C2-C3 area using PC-MRI in a cohort of cognitively normal young adults, to determine the feasibility of investigating CSF and CBF flow dynamics.

METHODS

Participants

Twenty-seven healthy, cognitively normal young adults (age 24.8±3.9 years; range 20–35 years of age; 14 females) provided written consent to participate in this study, which was approved by the institutional review board and performed in accordance with the 1964 Declaration of Helsinki. Participants were selected from a convenience sample of local students and staff. Subjects with MRI contraindications, psychiatric illness, and neurological disorders were excluded from the study.

Image Acquisition

Flow measurements were acquired on a 3T Siemens Prisma MRI machine using a 2D cine-PC pulse sequence with flow compensation. MRI parameters, derived from previous studies assessing CSF and CBF flow[17], were optimized and set as follows: 32 frames per cardiac cycle; 140×140 mm^2 field of view; 25° flip angle; 60% phase oversampling; 336×336 matrix with interpolation and fractional echo readout; 5 mm slice thickness; 201 Hz/Px receiver bandwidth; 1 NEX; TR/TE – 27.06/8.55 ms (cerebral aqueduct, C2-C3 vascular vessels),

28.02/9.03 ms (C2-C3 subarachnoid space). The TR duration represented a combination of flow compensation + flow encoding. All gradients were played at full strength (40 mT/m). For each segment, a single k-space line was collected. The encoding velocity was set to 10 cm/s for the cerebral aqueduct, 5 cm/s for the C2-C3 subarachnoid space, and 80 cm/s for the C2-C3 vascular vessels. A sagittal scout image was used as a localizer, and a T1 MP-RAGE image was acquired to select anatomical views for flow quantification. Acquisition planes were perpendicular to the direction of flow, with the cerebral aqueduct and C2-C3 area each being acquired in separate orthogonal planes. A peripheral pulse transducer was placed on the participant's finger for retrospective cardiac gating during acquisition. For every participant, three consecutive measurements were acquired at each region of interest to be included in the test-retest reliability assessment. PC-MRI data was acquired when the participant was at rest with a steady-state heart rate.

Regions of Interest

Two regions of interest were assessed for test-retest reliability (Figure 1): the cerebral aqueduct (CA) and C2-C3 area. Within the C2-C3 area, flow was measured at the left and right internal carotid arteries (ICA), vertebral arteries (VA), internal jugular veins (IJV), and subarachnoid space (SS). These ROIs were selected due to their utilization in several prior studies of CSF and CBF flow dynamics[17,38,40,41], suggesting these areas are potentially sensitive to the pathological changes that occur in neurological disease.

ROI Segmentation

All post-processing for test-retest reliability was performed by a biomedical engineering PhD student with 18 months of experience in PC-MRI and ROI segmentation. For evaluating inter-rater reliability, an MD / PhD student was trained for 2 hours over the course of one day on segmenting the ROIs at the CA and C2-C3 area. Segmentation for analysis of test-retest reliability was performed on a rolling basis as participants were imaged over the course of 18 months. Segmentation for intra-rater and inter-rater reliability analysis was performed over the course of 2 weeks. Post-processing took approximately 1.5 hours per participant and included ROI segmentation, generation of flow curves, extraction of flow parameters, and statistical analysis of reliability.

Flow curves were generated for the CA, SS, ICA, VA, and IJV regions using BioFlow v3.1.2, a free medical imaging analysis software with semi-automated segmentation capabilities.[42] However for this study, each region of interest was identified and manually traced as it was quicker and yielded similar ROI masks to the semi-automated segmentation routine, which often required altering the thresholding settings to avoid inclusion of pixels outside the practical boundaries of the ROI. A single ROI mask was applied across each of the 32 timeframes. The type of image used for segmentation varied based on the ROI and was set as follows: CA – complex difference (Figure 2), C2-C3 SS – phase (Figure 3), C2-C3 vascular vessels – magnitude (Figure 4). The image types for each ROI were chosen based on which provided the best pixel intensity contrast between flow and zero-flow pixels upon visual inspection.

Background Correction

To account for null background offsets due to imperfect suppression of eddy currents during acquisition, a background correction was applied to all flow curves generated at the CA and C2-C3 area. For the CA, a C-shaped mask with an inner radius twice the ROI diameter and an outer radius three times the ROI diameter was applied at the midbrain just above the ROI (Figure 2).[35,43] A C-shaped mask located above the ROI was chosen instead of a circular mask as this method has been shown in previous studies to be more reproducible.[43] Once the mask was applied, a background flow curve was generated and a point-by-point subtraction was performed on the CA flow curve. This was done to account for any time-based changes in background noise, as the mask was applied proximal to the ROI in an area with tissue and non-zero flow. For the C2-C3 area, a circular mask with a diameter approximately equivalent to that of the IJV ROI was applied at the center of the C2 posterior spinous process (Figure 3, Figure 4). As this is a known region of zero-flow, the resulting background flow curve was averaged, and the mean value was subtracted from each of the SS, ICA, VA, and IJV flow curves.

Calculation of Flow Parameters

The flow parameters analyzed in this study were derived from previous studies of CSF and CBF flow dynamics. All temporal delay parameters were calculated in %CC, a measure indicating the time in the cardiac cycle in which the flow measurement occurred relative to the total time of the heartbeat. For each flow curve, there were 32 flow measurements representing one cardiac cycle.

The ICA and VA flow curves were summed to create an arterial flow curve, while the venous flow curve was represented as the IJV flow curve. While the IJV is the primary pathway for venous outflow in the supine position, there are also contributions from the vertebral, epidural, and deep cervical veins.[44] As such, the IJV is only responsible for a percentage of the total venous outflow. To ensure that the arterial and venous flow curves were of the same scale, a correction factor was applied in which the ratio of average arterial flow to average venous flow was multiplied by each of the 32 flow values in the venous flow curve[17]. The arterio-venous flow curve (Figure 5E) was constructed as the summation of the arterial (Figure 5C) and corrected venous (Figure 5D) flow curves.

The zero-time reference for each flow curve represented the time in which the cardiac cycle was at peak systole as observed by the peripheral pulse transducer. However, due to transit time differences for blood between the heart, finger, and carotid artery, the arterial flow curve's zero-time point did not reflect the actual time in which cardiac peak systole occurred.

The CA (Figure 5A) and SS (Figure 5B) flow curves were integrated to yield stroke volume (mm^3), which represents the total displacement of CSF in the rostral and caudal direction over the cardiac cycle.[5,8,42,45,46] The maximum and minimum points on the flow curve were used to represent the flush and fill peak (mm^3/s), respectively.[41,45,47,48] The delay between the beginning of the flow curve and the maximum and minimum points were represented as the time-to-flush and time-to-fill peak (%CC), respectively.[42,47,48]

Arterial pulsatility (mm^3/s^2) was calculated as the slope of the arterial flow curve during systole.[17] Pulsatility index was calculated as the difference in systolic and diastolic peak flow over the mean flow rate.[32,49,50] Resistivity index was calculated as the difference in systolic and diastolic peak flow over systolic peak flow.[32,50] Pulse volume (mm^3) was calculated as the integration of the arterial flow curve over the period in which systole occurred.[17] The minimal and maximal points along the arterial and venous flow curve were represented as the systolic and diastolic peak (mm^3/s), respectively.[41,51] The delay between the beginning of the flow curves and the minimum and maximum points were represented as the time-to-systolic and time-to-diastolic peak (%CC), respectively.[41] Finally, the average of all 32 flow values on the arterial and venous flow curves was used to represent the average arterial flow and average venous flow, respectively.[38]

The arterio-venous flow curve was integrated to yield stroke volume (mm^3), which represents the total amount of blood displaced in the caudal direction of the cardiac cycle.[5,17] The time difference between the minimum arterial and maximum venous flow curve values was used to represent the arterio-venous delay (ms).[5,17]

Reliability Measurements

Test-retest reliability for each flow parameter was evaluated using the intraclass correlation coefficient (ICC) and coefficient of variance.[52,53] The ICC (3,1) two-way mixed ANOVA model in SPSS (IBM v24, 2016)[54] was used in this analysis to estimate the correlation between measurements for each flow parameter.[52] The participants and PC-MRI were both treated as fixed effects when assessing reliability. The reliability of each flow parameter was characterized as excellent (ICC ≥ 0.80), good (ICC 0.60 – 0.79), moderate (ICC 0.40 – 0.59), fair (ICC 0.20 – 0.39), or poor (ICC < 0.20).[55] Test-retest reliability was also assessed using coefficient of variation (CV), defined as the standard deviation of a group of measurements normalized to the mean of the group. The CVs for all participants were averaged for each flow parameter.

Intra-rater and inter-rater reliability of ROI segmentation during post-processing was also assessed for both CSF and CBF flow in a subset of 10 randomly selected participants. The cerebral aqueduct and all C2-C3 vascular ROIs were selected and manually traced three times for each participant in a randomized manner over multiple sessions. ICC was used to evaluate the intra-rater and inter-rater reliability for the 5 aqueductal and 14 vascular flow parameters.

RESULTS

Mean, standard deviation and test-retest reliability (ICC, CV%) values for all parameters analyzed at the CA and C2-C3 ROIs are shown in Table 1. Intra-rater and inter-rater reliability (ICC) values for the CA and C2-C3 vascular parameters analyzed are shown in Table 2.

Cerebral Aqueduct

Test-retest reliability for the CSF flow parameters analyzed in the CA ROI are shown in Figure 6A. All CSF flow parameters in this region reported an ICC>0.93, which is

considered excellent reliability, as well as a CV≤10%, except for flush peak (CV=11%). Intra-rater reliability and inter-rater reliability were excellent with an ICC=0.99 for all CSF flow parameters.

C2-C3 Area

Test-retest reliability for the CSF flow parameters analyzed in the C2-C3 SS ROI are shown in Figure 6B. Time-to-fill peak had an ICC=0.75, which is considered good reliability, and a CV=16%. The remaining CSF flow parameters in this region reported an ICC>0.94 and a CV≤10%, except for fill peak, with a CV=12%.

Figures 6C and 6D show the CBF flow parameters analyzed in the C2-C3 vascular ROI. Diastolic peak had good reliability with an ICC=0.70 and a CV=12%. Average arterial flow also had good reliability with an ICC=.79, but with a lower CV=9%. Pulsatility, pulsatility index, and pulse volume each had excellent reliability with an ICC=0.80, ICC=0.85, and ICC=0.88, respectively. However, the CVs for these parameters were moderate at 22%, 14%, and 14%, respectively. All remaining arterial flow parameters had excellent reliability and a CV≤10%. All venous flow parameters had excellent reliability with an ICC≥0.80 and a corresponding CV≤10%, except for systolic peak which had good reliability at an ICC=0.78. Intra-rater reliability and Inter-rater reliability was excellent with ICC>0.93 for all arterial and venous CBF flow parameters, except for pulsatility with an intra-rater ICC=0.87.

Figure 6E shows the arterio-venous flow parameters analyzed in the C2-C3 vascular ROI. From this flow curve, both stroke volume and arterio-venous delay had excellent reliability with an ICC=0.89. However, arterio-venous delay had a much higher CV=27% compared to stroke volume with a CV=14%.

DISCUSSION

The CSF and CBF flow parameters analyzed in this study generally had excellent test-retest reliability. The CSF flow parameters that measured flow rate (flush peak, fill peak), temporal delays (time-to-flush peak, time-to-fill peak), and volume (stroke volume) all had excellent reliability (ICC≥0.93). The single exception was time-to-fill peak for the SS which had good reliability (ICC=0.75). Similarly, CBF flow rate (systolic peak, diastolic peak, average venous flow, average arterial flow), temporal delays (time-to-systolic peak, time-to-diastolic peak), pulsatility (pulsatility index, resistivity index, pulsatility), and volume (arterio-venous stroke volume, pulse volume) generally had excellent reliability. The exceptions were arterial diastolic peak, average arterial flow, and venous systolic peak, which all had good reliability (ICC 0.70–0.79). Overall, the flow rate, temporal, pulsatility, and volume parameters all showed low variability.

Test-retest reliability, on a subset of the CSF and CBF flow parameters analyzed in our study, has been reported in other studies. One such study used PC-MRI to evaluate test-retest reliability of stroke volume and mean flow rate at the CA and C2-C3 region and reported excellent reliability similar to our study, but did not analyze temporal parameters, which are important measures for understanding the dynamic interplay between CSF and CBF flow in the brain.[27] In a similar study, good reliability was found for CSF flow rate and temporal

parameters, but were only evaluated for the CA.[36] In a study of CBF dynamics, short-term, long-term, and post-processing reliability of total cerebral blood flow measurements showed excellent reliability.[37]

The flow parameters described in our study have been used to evaluate the effects of pathological changes in the brain's drainage pathways and circulatory system. The brain is contained within a rigid skull and composed of tissue, CSF, and blood. According to the Monro-Kellie doctrine, any volume change in one intracranial component requires a compensatory change in another.[39] During systole, there is arterial inflow into the brain which initiates a cascade of outflow through the subarachnoid space, veins, and ventricles to maintain homeostatic pressure in the cranium.[56] The first step in the cascade is cranio-caudal CSF flush through the cervical subarachnoid space, followed by venous outflow, and finally cranio-caudal CSF flush through the cerebral aqueduct.[39] The temporal parameters described in this study can be used to measure the time-course of flow through the brain and potentially detect any abnormalities in the relationship between CSF and CBF flow in this cascade. Many studies have utilized these temporal flow parameters to study CSF and CBF flow dynamics in conditions of hydrocephalus[40,57] and normal aging[41].

Flow rate and volume parameters have also shown great utility in past studies. In one such study, significantly higher arterial pulsatility, pulse volume, and arterio-venous stroke volume were found in individuals with MCI when compared to normal older adults.[17] The study posited that the hyperdynamic arterial flow in MCI was due to degeneration of the arterial walls leading to changes in the regulation of arterial input.[17] In another study, decreased stroke volumes were reported in healthy older adults at the CA and cervical SS when compared to healthy young adults.[41] The study theorized that the lower flow volumes were due to abnormal changes in the resistance and compliance of the cervical and aqueductal compartments.[41] Aqueductal stroke volume has also been shown to have prognostic value in symptom progression and responsiveness to shunting in normal pressure hydrocephalus.[8,58] One related study proposed the ratio of aqueductal to subarachnoid stroke volume, measuring the distribution of flow between the CA and C2-C3 spaces, to be a strong indicator of flow dysfunction in patients with hydrocephalus.[59]

While our study and many of the previous studies described above utilized a 2D cine-PC pulse sequence to measure flow dynamics, PC-MRI has recently been expanded to measure flow in 3D as well. This technique, known as 4D flow MRI, encodes velocity along the 3-orthogonal spatial axis (x, y, z) allowing for a volumetric reconstruction of flow within a vessel.[60] Though 4D flow MRI is a relatively new technique, it has been utilized in several studies to evaluate flow dynamics in patients with clinical pathologies. In one such study, 4D flow MRI was used to evaluate group differences in mean blood flow, pulsatility, and mean transit time at the internal carotid artery, middle cerebral artery, superior sagittal sinus, and transverse sinus among individuals with AD, MCI, and those who were cognitively normal.[61] In another study, this technique was used to measure peak CSF flow at the cranio-cervical junction and cervical spinal canal in healthy individuals and those with Chiari malformations.[47] However, while 4D flow MRI has shown great promise in understanding flow dynamics, long scan times (5–20 minutes) and poor spatial resolution need to be addressed before it can be used as a routine clinical tool.[62]

Our study reports a comprehensive evaluation of the test-retest reliability of the different types of flow parameters which have been shown to be biologically relevant for understanding health and disease. However, our study does have a few notable limitations. First, the participants in this study are all healthy, young adults. It is possible that a similar study in older individuals with pathological conditions would yield greater variability in the flow parameters analyzed at the CA and C2-C3 area. Second, while we visually ensured that the acquisition plane was perpendicular to the presumed direction of flow at the cerebral aqueduct and C2-C3 area, physiological variations in positioning of the vessels through these regions make it impossible to capture all flow directions. However, while this could lead to reduced accuracy of the flow measurements, the precision should remain relatively unaffected. Third, using a peripheral pulse transducer to synchronize data acquisition to the cardiac cycle is known to be less reliable than ECG, as the ECG's sharp R-wave peak can be more reliably identified than the broad peak from an O2 saturation signal. It is possible this could result in lower reliability in temporal-based flow parameters. However, this did not affect our temporal parameters, which generally had excellent test-retest reliability.

An additional limitation is that our study only assessed test-retest reliability during a single session with each repeat scan utilizing the same localizer. Additional variability could be introduced if repeat measurements are taken after acquiring a new localizer scan following repositioning of participants on the scanner. This variability could also increase if the measurements are taken across multiple days. However, in one study on PC-MRI reproducibility, total cerebral blood flow measurements reported a CV ≤ 11% regardless of whether the repeat scan was acquired after subject repositioning or on a different day.[37] In another study by Luetmer et al.[35], mean flow rate at the CA reported a CV < 9% for three repeated measurements taken on different scanners over 2 weeks. Since the goal of our study was to evaluate reliability over time within a single session, additional studies are needed to investigate the effects of day-to-day variability and subject repositioning on the flow parameters described in this study.

While the limitations described above can affect test-retest reliability, accurate and consistent ROI segmentation during post-processing is also a significant factor. In our study, manually tracing the ROIs required visual inspection and subjective determinations of the lumen boundaries which were sometimes blurred by motion artifacts and partial volume effects. The aqueduct was particularly challenging, as any inaccuracies in boundary identification can significantly affect the flow measurements due to its relatively small size. However, inter-rater and intra-rater reliability was excellent at this region, suggesting that these sources of error did not substantially affect the reliability of boundary identification.

While segmentation of the CA was challenging due to its small size, the C2-C3 SS was also challenging because of its complex ring shape and low intensity contrast between flow and zero-flow pixels. However, because of its large surface area, small errors in boundary identification likely had a minimal effect on the results. This is further confirmed by the excellent inter-rater and intra-rater reliability in this region.

The C2-C3 vascular vessels were the most challenging region to segment due to the vessel's movement throughout the cardiac cycle. This required the ROI mask to be applied such that

it encapsulated the entire boundary of the vessel across all image slices. However, the proximity of the ICA and IJV vessels made it difficult to ensure that the mask for one ROI did not overlap onto another. Due to these challenges, the flow parameters in this region had the lowest test-retest, intra-rater and inter-rater reliability. Moreover, since the flow parameters in this region were based on summed arterial and venous flow curves, boundary identification errors at each vessel accumulated.

Another approach to the post-processing analysis is using time-resolved segmentation instead of applying a single ROI mask across all slices. Time-resolved segmentation is a technique in which a separate ROI mask is applied across each image slice, reducing the probability of including pixels outside the vessel boundary, such as those within an adjacent ROI or stationary tissue. This could improve accuracy and reliability in the CBF flow measurements but will also result in significantly higher post-processing times which might not be practical in many settings such as the clinic. It may also not be as necessary with the vessels in the brain, which have a smaller amount of displacement over the cardiac cycle than the larger cardiovascular vessels proximal to the heart.

Despite the post-processing challenges described above, all parameters analyzed in our study showed excellent intra-rater and inter-rater reliability. These findings are supported by previous studies looking at intra-rater and inter-rater reliability in a subset of CSF and CBF flow parameters. In one study looking at repeatability of aqueductal CSF flow measurements, both intra-rater and inter-rater variability were shown to be lower than inter-trial variability.[35] This was confirmed in another study on CSF flow, where aqueductal stroke volume, peak mean velocity, and peak systolic velocity, parameters commonly used in the literature, all had high intra-rater and inter-rater reliability (ICC > .88).[45] In a similar study looking at CBF flow measurement reliability at the carotid and vertebral arteries, inter-rater variability was again shown to be lower than inter-trial variability.[63] In another study looking at repeatability of CSF and CBF flow at the C2 cervical level, high intra-rater and inter-rater reliability was reported and it was also shown that experience level of the rater had a negligible influence on variability.[64] Overall, this suggests that inter-rater and intra-rater variance are not significant contributors to the overall variance between trials.

In addition to ROI segmentation during post-processing, there are also other physiological factors that can influence CSF and CBF flow dynamics and subsequently, test-retest reliability. These include physiological factors such as heart rate[15], respiration[65,66], and diurnal variations due to the body's circadian system.[67] Dietary intake of caffeine has also been shown to influence cerebral blood flow.[68] In a study on test-retest reliability of CBF flow, it was shown that venous flow at the internal jugular veins had greater variability than carotid arterial flow due to its sensitivity to body position, head position, hydration levels, and respiratory rate.[69] This variability can also be attributed to the higher flexibility and collapsibility of the internal jugular veins relative to the internal carotid artery.[44] Furthermore, when the participant is in a supine position, the left brachiocephalic vein can undergo severe narrowing resulting in temporary retrograde flow of the left jugular vein.[70,71] Taken together, these physiological effects can often result in the appearance of partial or missing jugular vein lumens, as well as bi-directional flow on an image acquired with PC-

MRI.[44] These possibilities need to be taken into consideration when evaluating flow at the internal jugular vein in healthy individuals and those with pathological conditions.

In this study we have shown that flow rate, volume, pulsatility, and temporal parameters can be measured and calculated with good repeatability at the CA and cervical C2-C3 area, regions commonly studied in health and disease, using PC-MRI. However, despite technological advances in the suppression of eddy currents, concomitant gradients, and gradient non-linearities, as well as improvements in the post-processing pipeline, there are still systematic sources of error that cannot be accounted for which can affect the accuracy of these flow measurements. Moreover, since accuracy has also shown to be dependent on vessel size and flow rate, these systematic errors can affect each flow region of the brain differently.[34] Furthermore, as there is no non-invasive gold standard for measuring cerebrovascular flow, it is difficult to evaluate the magnitude of the flow bias relative to the true physiological flow rates.

These accuracy issues need to be addressed to establish PC-MRI as a clinically useful tool for measuring CSF and CBF flow dynamics. One option is to establish normative values for the CSF and CBF flow parameters based on criteria such as age, ethnicity, gender, and pathology, to be used as a standard for comparison. In a clinical setting, a patient's flow measurements can then be compared to normative values to assist in diagnosis. Another option is to establish a baseline measurement of flow dynamics in a patient which can then be used to evaluate treatment effects or disease progression over time.

Overall, identifying a non-invasive biomarker of flow dynamics has broad implications across several diseases that are associated with CSF and CBF dysfunction, such as Alzheimer's disease, MCI, and communicating hydrocephalus. Future steps in establishing flow dynamics as a non-invasive biomarker include standardizing post-processing analysis to reduce complexity and processing time, educating practitioners on the clinical utility of measuring CSF and CBF flow dynamics, and continuing to identify the appropriate clinical populations who may benefit.

ACKNOWLEDGEMENTS

We thank Drs. Lirong Yan, Meng Law, Soroush Pahlavian, Jin Jin, and Danny JJ Wang for providing feedback on image analysis, and James Stanis for assistance with image rendering.

Funding Sources:

This work was supported by the National Institutes of Health (R01-AG054617, R01-AG046928, P41-EB015922).

REFERENCES

1. Attwell D, Buchan AM, Charpak S, Lauritzen M, MacVicar BA, Newman EA. Glial and neuronal control of brain blood flow. Nature 2010;468(7321):232–243. 10.1038/nature09613 [PubMed: 21068832]
2. Simon MJ, Iliff JJ. Regulation of cerebrospinal fluid (CSF) flow in neurodegenerative, neurovascular and neuroinflammatory disease. Biochimica et Biophysica Acta (BBA) - Molecular Basis of Disease 2016;1862(3):442–451. 10.1016/j.bbadis.2015.10.014 [PubMed: 26499397]

3. Tarasoff-Conway JM, Carare RO, Osorio RS, et al. Clearance systems in the brain [mdash] implications for Alzheimer disease. Nature Reviews Neurology 2015;11(8):457–470. [PubMed: 26195256]
4. Battal B, Kocaoglu M, Bulakbasi N, Husmen G, Tuba Sanal H, Tayfun C. Cerebrospinal fluid flow imaging by using phase-contrast MR technique. Br J Radiol 2011;84(1004):758–765. 10.1259/bjr/66206791 [PubMed: 21586507]
5. Qvarlander S, Ambarki K, Wåhlin A, et al. Cerebrospinal fluid and blood flow patterns in idiopathic normal pressure hydrocephalus. Acta Neurol Scand 2017;135(5):576–584. 10.1111/ane.12636 [PubMed: 27388230]
6. Bateman GA, Loiselle AM. Can MR measurement of intracranial hydrodynamics and compliance differentiate which patient with idiopathic normal pressure hydrocephalus will improve following shunt insertion? Acta Neurochirurgica 2007;149(5):455–462. [PubMed: 17406777]
7. Greitz D, Hannerz J, Rähn T, Bolander H, Ericsson A. MR imaging of cerebrospinal fluid dynamics in health and disease: on the vascular pathogenesis of communicating hydrocephalus and benign intracranial hypertension. Acta Radiologica 1994;35(3):204–211. [PubMed: 8192953]
8. Bradley WG Jr, Scalzo D, Queralt J, Nitz WN, Atkinson DJ, Wong P. Normal-pressure hydrocephalus: evaluation with cerebrospinal fluid flow measurements at MR imaging. Radiology 1996;198(2):523–529. [PubMed: 8596861]
9. Vandertop WP. Syringomyelia. Neuropediatrics 2014;45(01):003–009. 10.1055/s-0033-1361921
10. Greitz D Unraveling the riddle of syringomyelia. Neurosurgical Review 2006;29(4):251–264. [PubMed: 16752160]
11. Ellenbogen RG, Armonda RA, Shaw DW, Winn HR. Toward a rational treatment of Chiari I malformation and syringomyelia. Neurosurgical Focus 2000;8(3):1–10.
12. Bhadelia RA, Bogdan AR, Wolpert SM, Lev S, Appignani BA, Heilman CB. Cerebrospinal fluid flow waveforms: analysis in patients with Chiari I malformation by means of gated phase-contrast MR imaging velocity measurements. Radiology 1995;196(1):195–202. [PubMed: 7784567]
13. Fernande PM, Dujovn M, Austrian JI, Charbel F, Mafee M, Alperin N. CSF quantitative MRI analysis in Chiari I malformation. Skull Base Surgery 1997;7(SUPPL. 1).
14. Sivaramakrishnan A, Alperin N, Surapaneni S, Lichtor T. Evaluating the effect of decompression surgery on cerebrospinal fluid flow and intracranial compliance in patients with Chiari malformation with magnetic resonance imaging flow studies. Neurosurgery 2004;55(6):1344–1351. [PubMed: 15574215]
15. Armonda RA, Citrin CM, Foley KT, Ellenbogen RG. Quantitative cine-mode magnetic resonance imaging of Chiari I malformations: an analysis of cerebrospinal fluid dynamics. Neurosurgery 1994;35(2):214–223; discussion 223–224. [PubMed: 7969828]
16. Gorucu Y, Albayram S, Balci B, et al. Cerebrospinal fluid flow dynamics in patients with multiple sclerosis: a phase contrast magnetic resonance study. Functional neurology 2011;26(4):215. [PubMed: 22364942]
17. El Sankari S, Gondry-Jouet C, Fichten A, et al. Cerebrospinal fluid and blood flow in mild cognitive impairment and Alzheimer's disease: a differential diagnosis from idiopathic normal pressure hydrocephalus. Fluids and Barriers of the CNS 2011;8(1):12. [PubMed: 21349149]
18. Lee VS, Spritzer CE, Carroll BA, et al. Flow quantification using fast cine phase-contrast MR imaging, conventional cine phase-contrast MR imaging, and Doppler sonography: in vitro and in vivo validation. AJR American Journal of Roentgenology 1997;169(4):1125–1131. [PubMed: 9308476]
19. Matsumae M, Hirayama A, Atsumi H, Yatsushiro S, Kuroda K. Velocity and pressure gradients of cerebrospinal fluid assessed with magnetic resonance imaging. Journal of Neurosurgery 2014;120(1):218–227. [PubMed: 23930855]
20. Coverdale NS, Gati JS, Opalevych O, Perrotta A, Shoemaker JK. Cerebral blood flow velocity underestimates cerebral blood flow during modest hypercapnia and hypocapnia. Journal of Applied Physiology 2014;117(10):1090–1096. [PubMed: 25012027]
21. Buonocore MH, Bogren H. Factors influencing the accuracy and precision of velocity-encoded phase imaging. Magnetic Resonance in Medicine 1992;26(1):141–154. [PubMed: 1625560]

22. Srichai MB, Lim RP, Wong S, Lee VS. Cardiovascular applications of phase-contrast MRI. American Journal of Roentgenology 2009;192(3):662–675. [PubMed: 19234262]
23. Lee VS, Spritzer CE, Carroll BA, et al. Flow quantification using fast cine phase-contrast MR imaging, conventional cine phase-contrast MR imaging, and Doppler sonography: in vitro and in vivo validation. AJR American Journal of Roentgenology 1997;169(4):1125–1131. [PubMed: 9308476]
24. Lotz J, Meier C, Leppert A, Galanski M. Cardiovascular flow measurement with phase-contrast MR imaging: basic facts and implementation. Radiographics 2002;22(3):651–671. [PubMed: 12006694]
25. Nayak KS, Nielsen J-F, Bernstein MA, et al. Cardiovascular magnetic resonance phase contrast imaging. Journal of Cardiovascular Magnetic Resonance 2015;17(1):71. [PubMed: 26254979]
26. Hoogeveen RM, Bakker CJ, Viergever MA. MR phase-contrast flow measurement with limited spatial resolution in small vessels: value of model-based image analysis. Magnetic Resonance in Medicine 1999;41(3):520–528. [PubMed: 10204875]
27. Wåhlin A, Ambarki K, Hauksson J, Birgander R, Malm J, Eklund A. Phase contrast MRI quantification of pulsatile volumes of brain arteries, veins, and cerebrospinal fluids compartments: repeatability and physiological interactions. Journal of Magnetic Resonance Imaging 2012;35(5): 1055–1062. [PubMed: 22170792]
28. Bernstein MA, Zhou XJ, Polzin JA, et al. Concomitant gradient terms in phase contrast MR: analysis and correction. Magnetic Resonance in Medicine 1998;39(2):300–308. [PubMed: 9469714]
29. Lorenz R, Bock J, Snyder J, Korvink JG, Jung BA, Markl M. Influence of eddy current, Maxwell and gradient field corrections on 3D flow visualization of 3D CINE PC-MRI data. Magnetic Resonance in Medicine 2014;72(1):33–40. [PubMed: 24006013]
30. Tao S, Trzasko JD, Gunter JL, et al. Gradient nonlinearity calibration and correction for a compact, asymmetric magnetic resonance imaging gradient system. Physics in Medicine & Biology 2016;62(2):N18. [PubMed: 28033119]
31. Stankovic Z, Allen BD, Garcia J, Jarvis KB, Markl M. 4D flow imaging with MRI. Cardiovascular Diagnosis and Therapy 2014;4(2):173. [PubMed: 24834414]
32. Harloff A, Albrecht F, Spreer J, et al. 3D blood flow characteristics in the carotid artery bifurcation assessed by flow-sensitive 4D MRI at 3T. Magnetic Resonance in Medicine 2009;61(1):65–74. [PubMed: 19097219]
33. Gach HM, Lowe IJ, Madio DP, et al. A programmable pre-emphasis system. Magnetic Resonance in Medicine 1998;40(3):427–431. [PubMed: 9727946]
34. Wentland AL, Wieben O, Korosec FR, Haughton VM. Accuracy and reproducibility of phase-contrast MR imaging measurements for CSF flow. American Journal of Neuroradiology 2010;31(7):1331–1336. [PubMed: 20203113]
35. Luetmer PH, Huston J, Friedman JA, et al. Measurement of cerebrospinal fluid flow at the cerebral aqueduct by use of phase-contrast magnetic resonance imaging: technique validation and utility in diagnosing idiopathic normal pressure hydrocephalus. Neurosurgery 2002;50(3):534–543. [PubMed: 11841721]
36. Bhadelia RA, Bogdan AR, Wolpert SM. Analysis of cerebrospinal fluid flow waveforms with gated phase-contrast MR velocity measurements. American Journal of Neuroradiology 1995;16(2):389–400. [PubMed: 7726089]
37. Spilt A, Box F, van der Geest RJ, et al. Reproducibility of total cerebral blood flow measurements using phase contrast magnetic resonance imaging. Journal of Magnetic Resonance Imaging 2002;16(1):1–5. [PubMed: 12112496]
38. Sundström P, Wåhlin A, Ambarki K, Birgander R, Eklund A, Malm J. Venous and cerebrospinal fluid flow in multiple sclerosis: A case-control study. Ann Neurol 2010;68(2):255–259. 10.1002/ana.22132 [PubMed: 20695018]
39. ElSankari S, Balédent O, Van Pesch V, Sindic C, De Broqueville Q, Duprez T. Concomitant analysis of arterial, venous, and CSF flows using phase-contrast MRI: a quantitative comparison between MS patients and healthy controls. Journal of Cerebral Blood Flow & Metabolism 2013;33(9):1314–1321. [PubMed: 23778162]

40. Gideon P, Ståhlberg F, Thomsen C, Gjerris F, Sørensen PS, Henriksen O. Cerebrospinal fluid flow and production in patients with normal pressure hydrocephalus studied by MRI. Neuroradiology 1994;36(3):210–215. [PubMed: 8041442]
41. Stoquart-ElSankari S, Balédent O, Gondry-Jouet C, Makki M, Godefroy O, Meyer M-E. Aging effects on cerebral blood and cerebrospinal fluid flows. Journal of Cerebral Blood Flow & Metabolism 2007;27(9):1563–1572. [PubMed: 17311079]
42. Balédent O, Idy-peretti I. Cerebrospinal fluid dynamics and relation with blood flow: a magnetic resonance study with semiautomated cerebrospinal fluid segmentation. Investigative Radiology 2001;36(7):368–377. [PubMed: 11496092]
43. Flórez YN, Moratal D, Forner J, et al. Semiautomatic analysis of phase contrast magnetic resonance imaging of cerebrospinal fluid flow through the aqueduct of Sylvius. Magnetic Resonance Materials in Physics, Biology and Medicine 2006;19(2):78.
44. Mancini M, Lanzillo R, Liuzzi R, et al. Internal jugular vein blood flow in multiple sclerosis patients and matched controls. PLoS One 2014;9(3):e92730. [PubMed: 24675965]
45. Tawfik AM, Elsorogy L, Abdelghaffar R, Naby AA, Elmenshawi I. Phase-contrast MRI CSF flow Measurements for the diagnosis of normal-pressure hydrocephalus: Observer agreement of velocity versus volume parameters. American Journal of Roentgenology 2017;208(4):838–843. [PubMed: 28140607]
46. Nitz WR, Bradley WG Jr, Watanabe AS, et al. Flow dynamics of cerebrospinal fluid: assessment with phase-contrast velocity MR imaging performed with retrospective cardiac gating. Radiology 1992;183(2):395–405. [PubMed: 1561340]
47. Bunck AC, Kroeger JR, Juettner A, et al. Magnetic resonance 4D flow analysis of cerebrospinal fluid dynamics in Chiari I malformation with and without syringomyelia. European Radiology; Heidelberg 2012;22(9):1860–1870. 10.1007/s00330-012-2457-7
48. Schroeder HW, Schweim C, Schweim KH, Gaab MR. Analysis of aqueductal cerebrospinal fluid flow after endoscopic aqueductoplasty by using cine phase-contrast magnetic resonance imaging. Journal of Neurosurgery 2000;93(2):237–244.
49. Stalder AF, Frydrychowicz A, Russe MF, et al. Assessment of flow instabilities in the healthy aorta using flow-sensitive MRI. Journal of Magnetic Resonance Imaging 2011;33(4):839–846. [PubMed: 21448948]
50. Rivera-Rivera LA, Turski P, Johnson KM, et al. 4D flow MRI for intracranial hemodynamics assessment in Alzheimer's disease. Journal of Cerebral Blood Flow & Metabolism 2016;36(10): 1718–1730. [PubMed: 26661239]
51. Marks MP, Pelc NJ, Ross MR, Enzmann DR. Determination of cerebral blood flow with a phase-contrast cine MR imaging technique: evaluation of normal subjects and patients with arteriovenous malformations. Radiology 1992;182(2):467–476. [PubMed: 1732966]
52. Shrout PE, Fleiss JL. Intraclass correlations: uses in assessing rater reliability. Psychological Bulletin 1979;86(2):420. [PubMed: 18839484]
53. Weber EU, Shafir S, Blais A-R. Predicting risk sensitivity in humans and lower animals: risk as variance or coefficient of variation. Psychological Review 2004;111(2):430. [PubMed: 15065916]
54. IBM Corp. Released 2016. IBM SPSS Statistics for Windows, Version 24.0 Armonk, NY: IBM Corp.
55. Guo CC, Kurth F, Zhou J, et al. One-year test–retest reliability of intrinsic connectivity network fMRI in older adults. Neuroimage 2012;61(4):1471–1483. [PubMed: 22446491]
56. Schroth G, Klose U. Cerebrospinal fluid flow. Neuroradiology 1992;35(1):16–24. [PubMed: 1289733]
57. Balédent O, Gondry-Jouet C, Meyer M-E, et al. Relationship between cerebrospinal fluid and blood dynamics in healthy volunteers and patients with communicating hydrocephalus. Investigative Radiology 2004;39(1):45–55. [PubMed: 14701988]
58. Scollato A, Tenenbaum R, Bahl G, Celerini M, Salani B, Di Lorenzo N. Changes in aqueductal CSF stroke volume and progression of symptoms in patients with unshunted idiopathic normal pressure hydrocephalus. American Journal of Neuroradiology 2008;29(1):192–197. [PubMed: 17925364]

59. Wagshul ME, Chen JJ, Egnor MR, McCormack EJ, Roche PE. Amplitude and phase of cerebrospinal fluid pulsations: experimental studies and review of the literature. Journal of Neurosurgery 2006;104(5):810–819. [PubMed: 16703889]
60. Stankovic Z, Allen BD, Garcia J, Jarvis KB, Markl M. 4D flow imaging with MRI. Cardiovascular Diagnosis and Therapy 2014;4(2):173. [PubMed: 24834414]
61. Rivera-Rivera LA, Schubert T, Turski P, et al. Changes in intracranial venous blood flow and pulsatility in Alzheimer's disease: A 4D flow MRI study. Journal of Cerebral Blood Flow & Metabolism 2017;37(6):2149–2158. [PubMed: 27492950]
62. Schnell S, Wu C, Ansari SA. 4D MRI flow examinations in cerebral and extracerebral vessels. Ready for clinical routine? Current Opinion in Neurology 2016;29(4):419. [PubMed: 27262148]
63. Peng S-L, Su P, Wang F-N, et al. Optimization of phase-contrast MRI for the quantification of whole-brain cerebral blood flow. Journal of Magnetic Resonance Imaging 2015;42(4):1126–1133. [PubMed: 25676350]
64. Koerte I, Haberl C, Schmidt M, et al. Inter-and intra-rater reliability of blood and cerebrospinal fluid flow quantification by phase-contrast MRI. Journal of Magnetic Resonance Imaging 2013;38(3):655–662. [PubMed: 23371821]
65. Dreha-Kulaczewski S, Joseph AA, Merboldt K-D, Ludwig H-C, Gärtner J, Frahm J. Inspiration is the major regulator of human CSF flow. Journal of Neuroscience 2015;35(6):2485–2491. [PubMed: 25673843]
66. Chen L, Beckett A, Verma A, Feinberg DA. Dynamics of respiratory and cardiac CSF motion revealed with real-time simultaneous multi-slice EPI velocity phase contrast imaging. Neuroimage 2015;122:281–287. [PubMed: 26241682]
67. Nilsson C, Ståhlberg F, Thomsen C, Henriksen O, Herning M, Owman C. Circadian variation in human cerebrospinal fluid production measured by magnetic resonance imaging. American Journal of Physiology-Regulatory, Integrative and Comparative Physiology 1992;262(1):R20–R24.
68. Addicott MA, Yang LL, Peiffer AM, et al. The effect of daily caffeine use on cerebral blood flow: How much caffeine can we tolerate? Human Brain Mapping 2009;30(10):3102–3114. [PubMed: 19219847]
69. Schrauben EM, Johnson KM, Huston J, et al. Reproducibility of cerebrospinal venous blood flow and vessel anatomy with the use of phase contrast–vastly undersampled isotropic projection reconstruction and contrast-enhanced MRA. American Journal of Neuroradiology 2013.
70. Jang J, Kim B, Kim B, et al. Reflux venous flow in dural sinus and internal jugular vein on 3D time-of-flight MR angiography. Neuroradiology 2013;55(10):1205–1211. [PubMed: 23868180]
71. Fushimi Y, Okada T, Okuchi S, Yamamoto A, Kanagaki M, Fujimoto K, & Togashi K (2016). Jugular venous reflux on magnetic resonance angiography and radionuclide venography. Acta Radiologica Oopen 2016;5(12):2058460116681209.

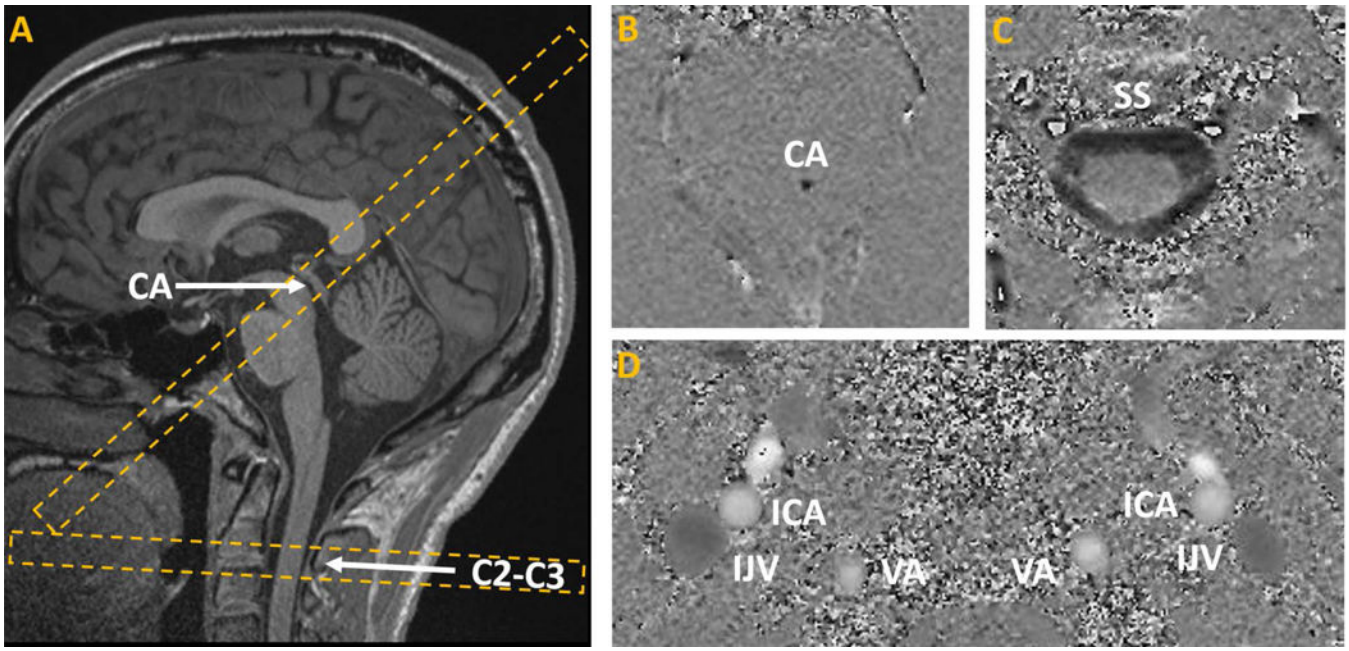

Figure 1:
Representative set of acquired images for a participant. **(A)** Structural T1 MPRAGE. The yellow dashed lines represent the acquisition planes, which were perpendicular to the direction of flow. **(B)** PC-MRI flow phase image at the cerebral aqueduct (CA), **(C)** subarachnoid space (SS), and **(D)** internal carotid artery (ICA), internal jugular vein (IJV), and vertebral artery (VA).

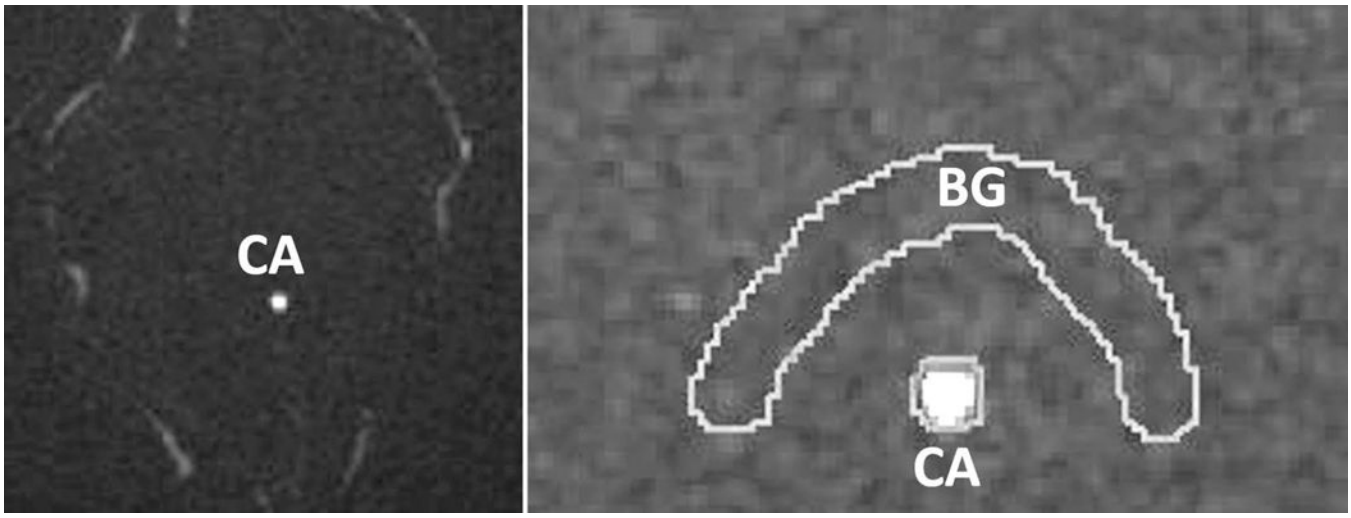

Figure 2:
(Left) Complex-difference image at the CA. **(Right)** Background correction (BG) and cerebral aqueduct (CA) masks applied to a complex difference image.

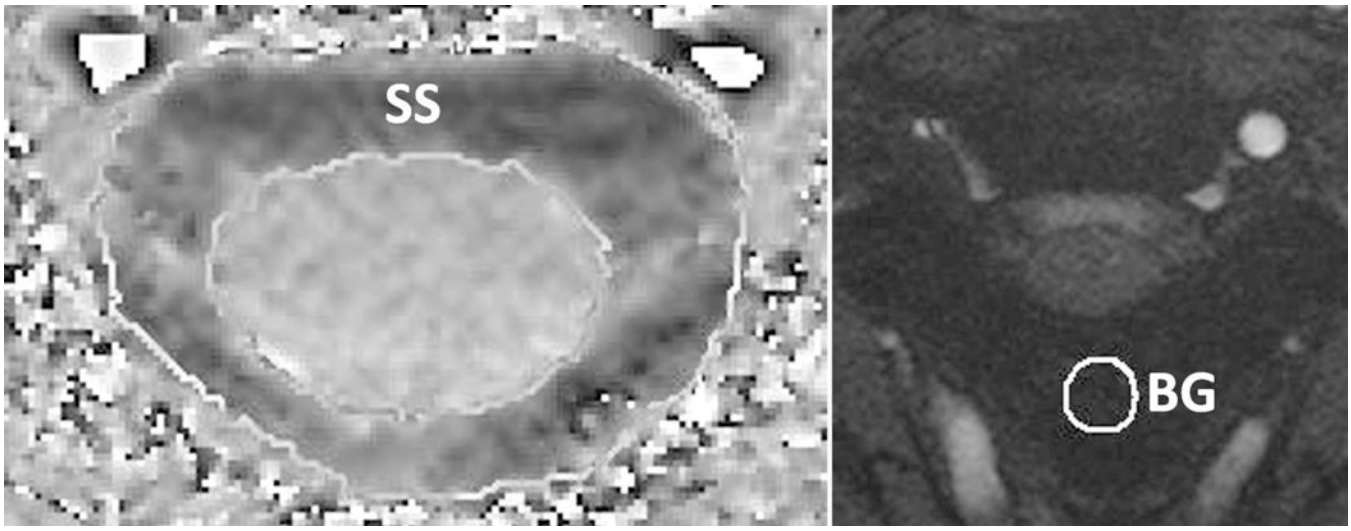

Figure 3:
(Left) Phase image with an applied mask at the C2-C3 SS. **(Right)** Circular background correction (BG) mask applied at the C2 posterior spinous process.

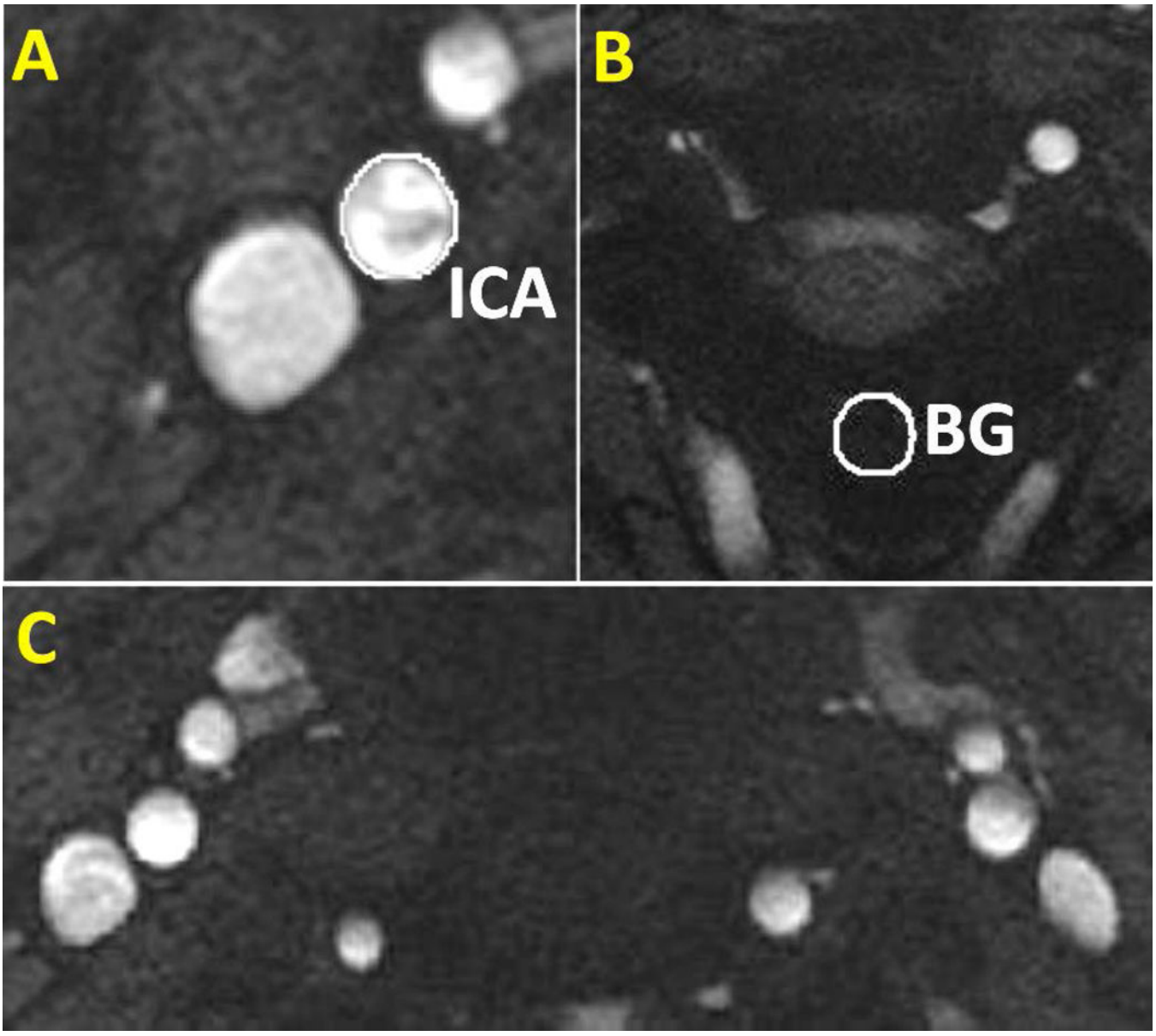

Figure 4:

(A) Example of a circular mask applied at the C2-C3 vascular ROIs, specifically at the right ICA. **(B)** Circular background correction (BG) mask applied at the C2 posterior spinous process. **(C)** Magnitude image of the C2-C3 vascular area containing the ICA, IJV, and VA

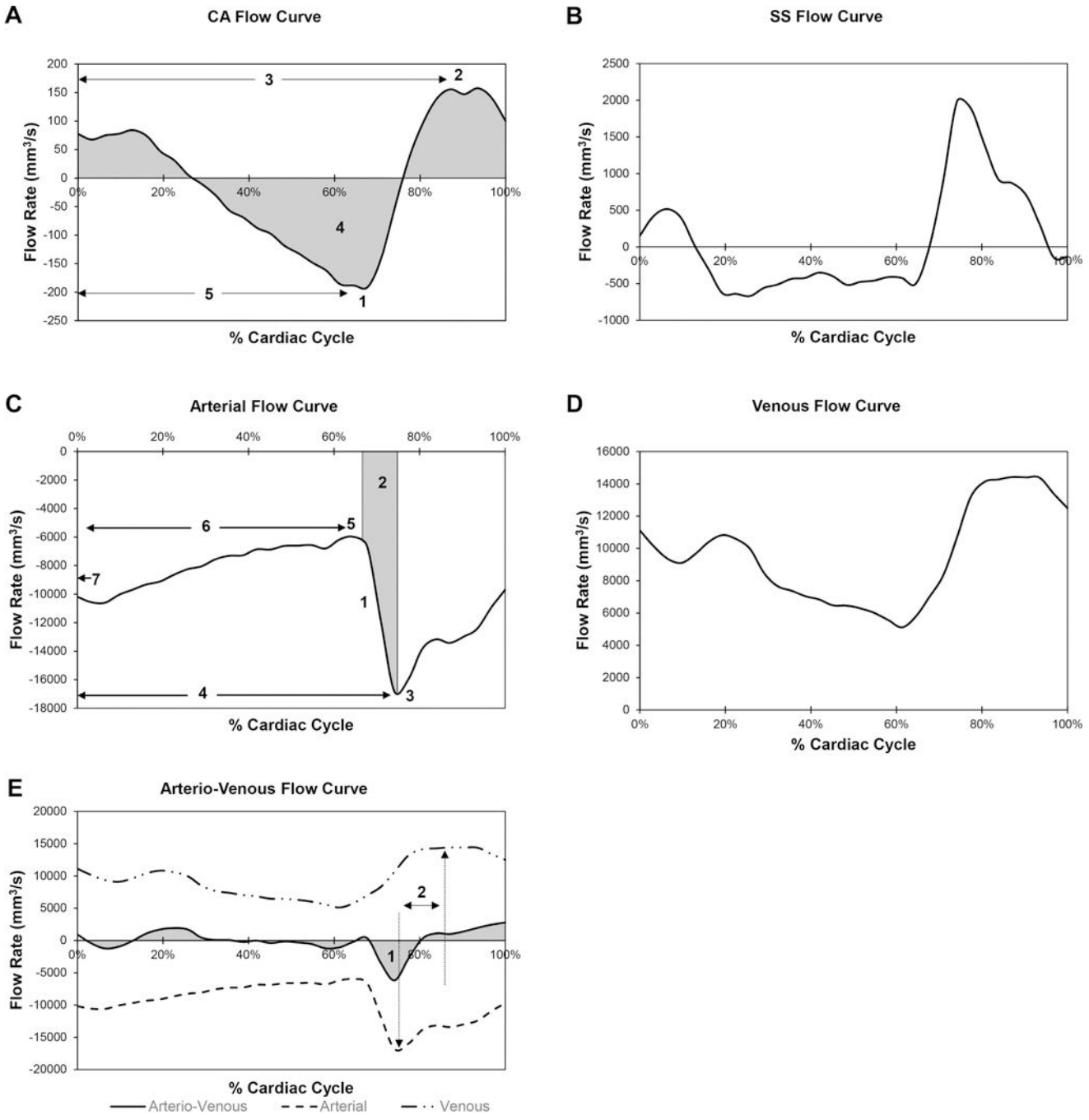

Figure 5:

Representative flow curves from one participant. **(A)** CA flow curve – 1. fill peak, 2. flush peak, 3. time-to-flush peak, 4. stroke volume, 5. time-to-fill peak; **(B)** SS flow curve – same flows parameters as CA flow curve; **(C)** arterial flow curve – 1. arterial pulsatility, 2. arterial pulse volume, 3. systolic peak, 4. time-to-systolic peak, 5. diastolic peak, 6. time-to-diastolic peak, 7. average flow, **(D)** venous flow curve – same flow parameters as arterial flow curve excluding arterial pulsatility and pulse volume, **(E)** arterio-venous flow curve – 1. stroke volume, 2. arterio-venous delay

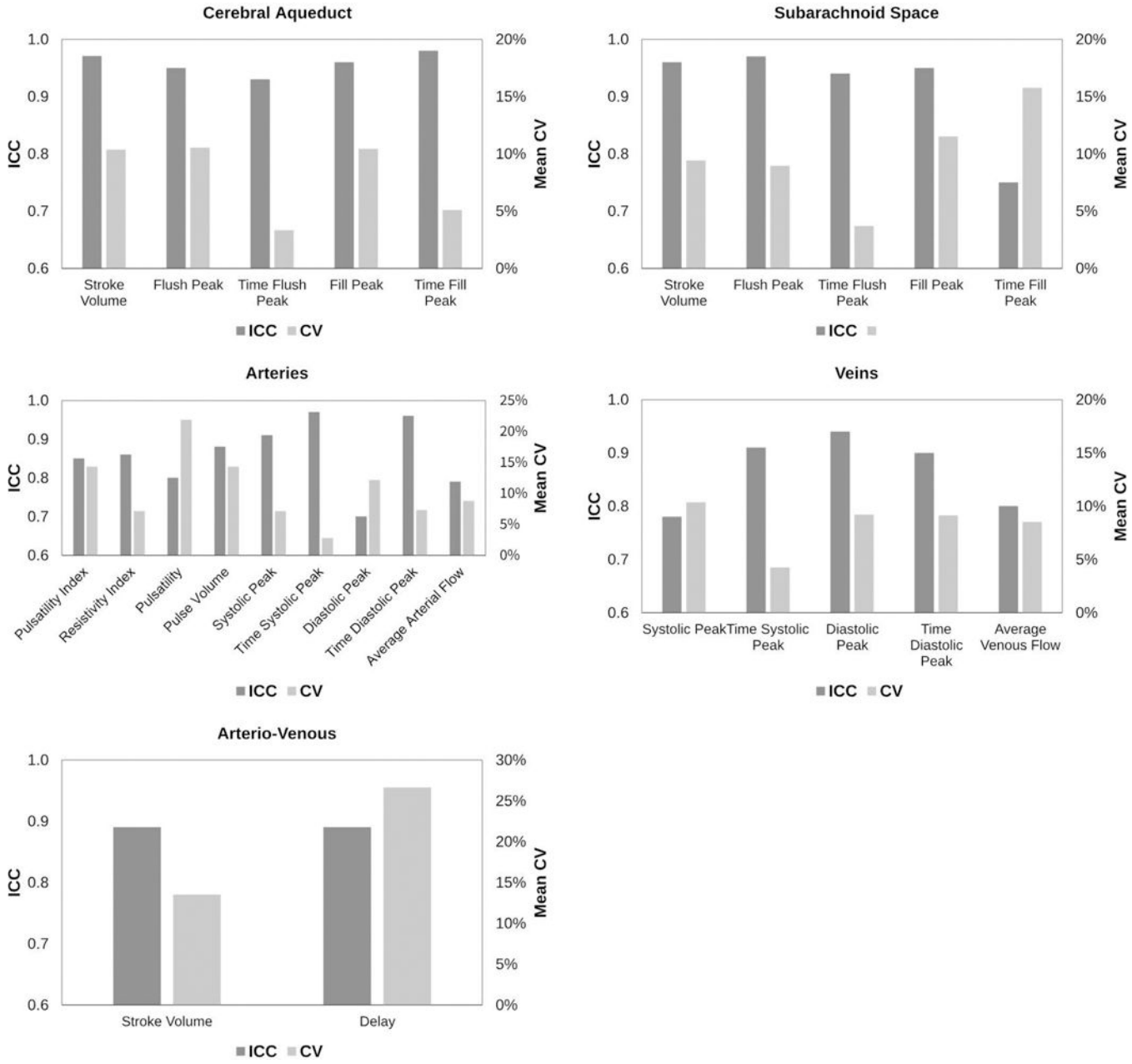

Figure 6:

(A-E) ICC and mean CV for the flow parameters calculated from the CA, SS, arterial, venous, and arterio-venous flow curves, respectively. Among the CSF flow parameters, CA stroke volume and time-to-fill peak had the highest ICC. Arterial time-to-systolic peak and time-to-diastolic peak had the highest ICC of the CBF flow parameters.

Table 1:

Test-retest reliability mean, standard deviation, ICC, and mean CV values for all flow parameters.

Region	Flow Parameter	Mean	SD	ICC	CV%
Cerebral Aqueduct	Stroke Volume (mm^3)	38	17	0.97	10%
	Flush Peak (mm^3/s)	129	42	0.95	11%
	Time Flush Peak (%CC)	87%	9%	0.93	3%
	Fill Peak (mm^3/s)	133	55	0.96	10%
	Time Fill Peak (%CC)	55%	15%	0.98	5%
Subarachnoid Space	Stroke Volume (mm^3)	649	222	0.96	9%
	Flush Peak (mm^3/s)	2799	981	0.97	9%
	Time Flush Peak (%CC)	76%	9%	0.94	4%
	Fill Peak (mm^3/s)	1803	599	0.95	12%
	Time Fill Peak (%CC)	48%	14%	0.75	16%
Arteries	Pulsatility Index	1.09	0.23	0.85	14%
	Resistivity Index	0.62	0.07	0.86	7%
	Pulsatility (mm^3/s^2)	106032	37815	0.80	22%
	Pulse Volume (mm^3)	758	259	0.88	14%
	Systolic Peak (mm^3/s)	19650	2902	0.91	7%
	Time Systolic Peak (%CC)	68%	9%	0.97	3%
	Diastolic Peak (mm^3/s)	7333	1369	0.70	12%
	Time Diastolic Peak (%CC)	52%	11%	0.96	7%
	Average Arterial Flow (mm^3/s)	10339	2135	0.79	9%
Veins	Systolic Peak (mm^3/s)	16101	2591	0.78	10%
	Time Systolic Peak (%CC)	80%	10%	0.91	4%
	Diastolic Peak (mm^3/s)	7696	2002	0.94	9%
	Time Diastolic Peak (%CC)	49%	12%	0.90	9%
	Average Venous Flow (mm^3/s)	10456	2147	0.80	9%
Arterio-Venous	Stroke Volume (mm^3)	811	223	0.89	14%
	Delay (%CC)	12%	6%	0.89	27%

Table 2:

Intra-rater and inter-rater reliability ICC values for CA, arterial, and venous flow parameters.

Region	Flow Parameter	Intra-Rater ICC	Inter-Rater ICC
Cerebral Aqueduct	Stroke Volume (mm^3)	0.99	0.99
	Flush Peak (mm^3/s)	0.99	0.99
	Time Flush Peak (%CC)	0.99	0.99
	Fill Peak (mm^3/s)	0.99	0.99
	Time Fill Peak (%CC)	0.99	0.99
Arteries	Pulsatility Index	0.96	0.98
	Resistivity Index	0.93	0.98
	Pulsatility (mm^3/s^2)	0.87	0.93
	Pulse Volume (mm^3)	0.94	0.97
	Systolic Peak (mm^3/s)	0.98	0.99
	Time Systolic Peak (%CC)	0.99	0.99
	Diastolic Peak (mm^3/s)	0.97	0.98
	Time Diastolic Peak (%CC)	0.99	0.99
	Average Arterial Flow (mm^3/s)	0.98	0.99
Veins	Systolic Peak (mm^3/s)	0.96	0.98
	Time Systolic Peak (%CC)	0.98	0.99
	Diastolic Peak (mm^3/s)	0.99	0.99
	Time Diastolic Peak (%CC)	0.99	0.99
	Average Venous Flow (mm^3/s)	0.99	0.99